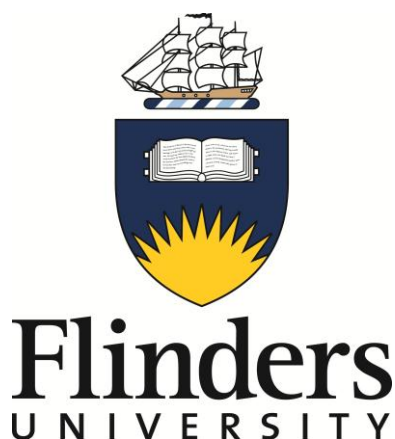


# Quantum dot and carbon dot polymer nanocomposites for latent fingerprint detection



A thesis submitted to the School of Chemical & Physical Sciences, Faculty of Science & Engineering, at The Flinders University of South Australia in fulfilment of the degree of

Doctor of Philosophy

March 2014

**Jessirie Dilag**

BTech (Forensic & Analytical Chemistry), BSc (Hons)

Supervisors: Professor Amanda V. Ellis,

Co-supervisors: Professor Hilton J. Kobus &

Professor Joseph G. Shapter

# Table of Contents

<b>Declaration.....</b>	<b>IX</b>
<b>Acknowledgements.....</b>	<b>X</b>
<b>Abstract.....</b>	<b>XI</b>
<b>Publications.....</b>	<b>XIII</b>
<b>List of figures.....</b>	<b>XV</b>
<b>List of tables.....</b>	<b>XXII</b>
<b>List of abbreviations, symbols, and units.....</b>	<b>XXIV</b>
<b>Thesis guide.....</b>	<b>XXVII</b>
<b>Chapter 1. Introduction.....</b>	<b>28</b>
1.1 Synopsis .....	28
1.2 Latent fingerprint detection .....	29
1.2.1 Composition of latent fingerprints.....	30
1.2.2 Surface types: Porous, non-porous, and semi-porous .....	30
1.2.3 Conventional methods of development.....	31
1.3 Fluorescent visual enhancement of developed fingerprints .....	33
1.4 Quantum dots (QDs) .....	34
1.4.1 Electronic properties of QDs.....	35
1.4.2 Optical properties of QD - absorbance and fluorescence.....	36
1.4.2.1 The hyperbolic band model .....	38
1.4.3 QD synthesis .....	40
1.4.4 QD surface protection – capping/stabilising agents .....	40
1.4.5 Experimental factors that affect QD size .....	42
1.5 QDs in fingerprint detection – Literature review.....	43
1.6 Toxicity – health concerns of QDs .....	49
1.7 Carbon dots (C-dots) .....	51
1.7.1 Physical synthetic routes .....	53

1.7.2	Wet chemical synthetic routes .....	54
1.7.3	Optical properties of carbon dots .....	55
1.7.3.1	Environmental factors that affect optical properties .....	58
1.7.4	Photo-stability and blinking .....	59
1.8	Nanoparticle-polymer nanocomposites .....	60
1.8.1	Synthesis of nanoparticle-polymer nanocomposites .....	60
1.9	Reverse addition fragmentation chain transfer (RAFT) polymerisation .....	61
1.9.1	RAFT chain transfer agents (CTAs) .....	62
1.9.2	Mechanism of RAFT polymerisation.....	63
1.9.3	Kinetics of RAFT polymerisation.....	64
1.9.4	RAFT end-group removal and functionalisation .....	65
1.10	Summary .....	67
1.11	References for Chapter 1 .....	69
<b>Chapter 2.</b>	<b>Experimental .....</b>	<b>79</b>
2.1	Synopsis .....	79
2.2	Materials.....	80
2.2.1	Table of chemicals and reagents .....	80
2.3	Synthetic procedures .....	82
2.3.1	Synthesis of CdS/2-mercaptoethanol QDs.....	82
2.3.2	Synthesis of CdS/C <sub>12</sub> CTA QDs .....	83
2.3.3	Surface initiated RAFT polymerisation .....	84
2.3.3.1	Synthesis of CdS/p(DMA).....	86
2.3.3.2	Synthesis of CdS/p(DMA- <i>co</i> -MMA) .....	86
2.3.3.3	Synthesis of CdS/p(DMA- <i>co</i> -Sty) .....	86
2.3.4	C-dot synthesis.....	87
2.3.5	Synthesis of the C-dot/polymer nanocomposites .....	88
2.3.5.1	Synthesis of C-dot/C <sub>12</sub> CTA .....	88
2.3.5.2	Synthesis of C-dot/p(DMA) .....	88
2.3.5.3	Synthesis of C-dot/p(DMA- <i>co</i> -MMA) .....	89

2.3.6	Synthesis of magnetic C-dot/p(DMA- <i>co</i> -MMA) and CdS/p(DMA- <i>co</i> -MMA) nanocomposite	89
2.3.6.1	One-pot aminolysis/thiol-ene click chemistry of C-dot/p(DMA- <i>co</i> -MMA) and CdS/p(DMA- <i>co</i> -MMA) to DVS-activated magnetic particles. ....	90
2.3.7	Ultra-Violet (UV) – visible (vis) spectrophotometry .....	91
2.3.7.1	UV-vis spectrophotometry sample preparation and data acquisition.....	92
2.3.7.2	Estimation of CdS QD diameter using the hyperbolic band model .....	92
2.4	Characterisation techniques.....	93
2.4.1	Fluorescence spectrophotometry.....	93
2.4.1.1	Sample preparation and instrumentation .....	93
2.4.1.2	Quantum yield (QY) determination.....	94
2.4.2	Dynamic light scattering (DLS) for C-dot size determination .....	95
2.4.3	Transmission electron microscopy (TEM) for CdS QD size determination .....	95
2.4.3.1	Sample preparation and instrumentation .....	96
2.4.4	X-ray photoelectron spectroscopy (XPS) analysis of C-dots.....	96
2.4.5	Raman spectroscopy analysis of C-dots.....	97
2.4.6	Nuclear magnetic resonance (NMR) spectroscopy.....	97
2.4.6.1	Sample preparation and instrumentation for <sup>1</sup> H NMR spectral analysis of RAFT polymers .....	98
2.4.6.2	Data acquisition and analysis for kinetic studies .....	98
2.4.6.3	Sample preparation and instrumentation for <sup>13</sup> C NMR spectral analysis of purified C-dots	99
2.4.7	Fourier transform infrared (FTIR) spectroscopy.....	100
2.4.7.1	Sample preparation and instrumentation .....	100
2.4.8	Gel permeation chromatography (GPC) .....	101
2.4.8.1	Sample preparation and instrumentation .....	101
2.4.9	Thermogravimetric analysis (TGA).....	102
2.4.9.1	Sample preparation and instrumentation .....	103
2.5	References for Chapter 2.....	104
<b>Chapter 3.</b>	<b>CdS/polymer nanocomposites.....</b>	<b>107</b>

3.1	Synopsis .....	107
3.2	Synthesis of CdS/2-mercaptoethanol.....	108
3.2.1	Absorbance (CdS bulk vs. CdS QDs) – the quantum confinement effect.....	109
3.2.1.1	UV-vis spectrophotometry and the hyperbolic band model .....	111
3.2.2	Precursor concentration effects .....	112
3.2.3	Size determination <i>via</i> TEM imaging .....	113
3.2.4	Fluorescence spectra of CdS/2-mercaptoethanol QDs.....	115
3.3	Synthesis of CdS/C <sub>12</sub> CTA QDs.....	117
3.3.1	Steglich esterification - Mechanism.....	118
3.3.2	Thermal and spectral analysis of CdS/2-mercaptoethanol QDs versus CdS/C <sub>12</sub> CTA QDs	121
3.3.2.1	Fourier transform infra-red (FTIR) spectral analysis.....	121
3.3.2.2	Thermogravimetric analysis (TGA).....	123
3.3.3	Optical properties of CdS/2-mercaptoethanol QDs versus CdS/C <sub>12</sub> CTA QDs..	125
3.4	Synthesis of CdS/p(DMA) <i>via</i> surface initiated RAFT polymerisation from CdS/C <sub>12</sub> CTA QDs	127
3.4.1	Experimental design of the RAFT polymerisation of DMA from CdS/C <sub>12</sub> CTA QDs	129
3.4.2	Monitoring the RAFT polymerisation of DMA from CdS/C <sub>12</sub> CTA QDs using <sup>1</sup> H NMR and FTIR spectroscopies.....	132
3.5	Synthesis of CdS/p(DMA- <i>co</i> -MMA) and CdS/p(DMA- <i>co</i> -Sty) powders .....	135
3.6	Characterisation of the RAFT polymers in the CdS/polymer nanocomposites.....	138
3.6.1	Monitoring the RAFT co-polymerisation of DMA with MMA and Sty, from CdS/C <sub>12</sub> CTA QD surfaces using <sup>1</sup> H NMR spectroscopy and GPC.....	138
3.6.1.1	<sup>1</sup> H NMR analysis of CdS/p(DMA- <i>co</i> -MMA).....	138
3.6.1.2	<sup>1</sup> H NMR analysis of CdS/p(DMA- <i>co</i> -Sty) .....	139
	GPC analysis of CdS/polymer nanocomposites.....	140
3.7	Kinetic studies for the RAFT polymerisation of DMA, MMA and Sty from the CdS/C <sub>12</sub> CTA QDs	141
3.7.1	TGA studies of CdS/polymer nanocomposites versus RAFT polymers without CdS QDs	142

3.8	Optical properties of the CdS/polymer nanocomposites .....	145
3.8.1	UV-vis absorbance spectra of CdS/polymer nanocomposites.....	146
3.8.2	Fluorescence emission spectra of CdS/polymer nanocomposites .....	147
3.8.2.1	Quantum yield (QY) of the CdS/polymer nanocomposites .....	149
3.9	Conclusion.....	150
3.10	References for Chapter 3.....	151
<b>Chapter 4.</b>	<b>C-dot/polymer nanocomposites .....</b>	<b>154</b>
4.1	Synopsis .....	154
4.2	Thermal oxidation of activated charcoal (AC).....	155
4.3	Physical and chemical properties of pristine C-dots.....	156
4.3.1	Raman spectroscopy .....	156
4.3.2	<sup>13</sup> C NMR spectroscopy of C-dots in D <sub>2</sub> O .....	158
4.3.3	FTIR spectroscopy of AC versus C-dots.....	159
4.3.4	XPS analysis of AC versus C-dots.....	160
4.3.5	C-dot nanoparticle size determined by dynamic light scattering (DLS) .....	162
4.4	Proposed structure of C-dots .....	162
4.5	C-dot optical properties .....	163
4.5.1	UV-vis absorbance of C-dots .....	164
4.5.2	Fluorescence of C-dots.....	166
4.5.3	Excitation wavelength.....	167
4.5.4	pH reversible fluorescence properties of C-dots .....	169
4.6	Synthesis of C-dot/p(DMA) nanocomposites.....	172
4.6.1	FTIR spectroscopy of the purified C-dots versus C-dot/C <sub>12</sub> CTA and C-dot/p(DMA) nanocomposite .....	172
4.6.2	TGA analysis of the C-dot/p(DMA) nanocomposites.....	174
4.6.3	GPC analysis of the C-dot/p(DMA) nanocomposites .....	175
4.6.4	<sup>1</sup> H NMR spectroscopy of the C-dot/p(DMA) nanocomposites.....	175
4.6.5	Kinetic plots of the C-dot/p(DMA) nanocomposite formation .....	177
4.6.6	Optical properties of the C-dot/p(DMA) nanocomposites .....	178

4.7	Conclusions .....	181
4.8	References for Chapter 4 .....	182

**Chapter 5. RAFT end-group post modification: Synthesis of magnetic nanocomposite powders 185**

5.1	Synopsis .....	185
5.2	One-pot aminolysis/click reaction .....	186
5.3	Characterisation of the magnetic nanocomposites .....	190
5.3.1	FTIR analysis of magnetic CdS/p(DMA- <i>co</i> -MMA)* and C-dot/p(DMA- <i>co</i> -MMA)* nanocomposites .....	191
5.3.2	TGA of the DVS-magnetic beads versus magnetic CdS/p(DMA- <i>co</i> -MMA)* and C-dot/p(DMA- <i>co</i> -MMA)* .....	194
5.3.3	UV-vis absorbance of the DVS-magnetic beads versus magnetic CdS/p(DMA- <i>co</i> -MMA)* and C-dot/p(DMA- <i>co</i> -MMA)* .....	197
5.3.4	Fluorescence spectra of DVS-magnetic beads versus magnetic CdS/p(DMA- <i>co</i> -MMA)* and C-dot/p(DMA- <i>co</i> -MMA)* .....	198
5.4	Visual observations: Photographs of the magnetic CdS/p(DMA- <i>co</i> -MMA)* nanocomposites 202	
5.5	Conclusions .....	204
5.6	References for Chapter 5 .....	205

**Chapter 6. Application of the CdS QD and C-dot polymer nanocomposites as fingerprint developing reagents..... 207**

6.1	Synopsis .....	207
6.2	Introduction and background information .....	208
6.2.1	Forensic light source – The Polilight® .....	209
6.2.2	Visualisation and photography .....	210
6.2.3	Ridge patterns of a fingerprint: Classification and minutiae .....	211
6.3	Preparation of the CdS QD and C-dot polymer nanocomposites as fingerprint reagents for latent fingerprint detection .....	213
6.3.1	Table of materials and reagents .....	213

6.4	Preparation of latent fingerprints .....	213
6.4.1	Surface substrates: Aluminium foil and glass microscope slides.....	214
6.5	Preparation of the CdS QD and C-dot polymer nanocomposite fingerprint reagents..	214
6.6	Visualisation and photography of the developed latent fingerprints .....	216
6.7	Photographs of the latent fingerprints developed by the CdS QD and C-dot polymer nanocomposites .....	216
6.7.1	Fingerprint development on aluminium foil substrates .....	217
6.7.1.1	Summary of observations for latent fingerprint detection on aluminium foil substrates	222
6.7.2	Fingerprint development on glass microscope slide substrates .....	223
6.7.2.1	Summary of observations for latent fingerprint detection on aluminium foil substrates	225
6.8	Fingerprint detection using the magnetic CdS/p(DMA- <i>co</i> -MMA)* powder nanocomposites	227
6.8.1	Table summarising the overall performance of the QD and C-dot polymer nanocomposites application in latent fingerprint detection.....	229
6.9	Conclusions .....	230
6.10	References for Chapter 6.....	231
<b>Chapter 7.</b>	<b>Conclusion and future research.....</b>	<b>232</b>
7.1	Summary .....	232
7.2	Concluding remarks .....	233
7.3	Future research .....	237
7.4	References for Chapter 7 .....	239
<b>Chapter 8.</b>	<b>Appendix.....</b>	<b>242</b>
8.1	Appendix A: <sup>1</sup> H NMR spectra of CdS/p(DMA- <i>co</i> -MMA) and CdS/p(DMA- <i>co</i> -Sty).	242
8.2	Appendix B: Photostability of CdS QDs over time (t = 2 months, 6, 12 and 18 months)	243





## Declaration

I certify that this thesis does not incorporate without acknowledgment any material previously submitted for a degree or diploma in any university; and that to the best of my knowledge and belief it does not contain any material previously published or written by another person except where due reference is made in the text.

---

Jessirie Dilag on \_\_\_\_\_

# Acknowledgements

The research presented in this thesis has been conducted at Flinders University, Adelaide, South Australia. Furthermore the project was funded by The Department of Justice of South Australia.

I am extremely grateful to my supervisor, Amanda Ellis, and co-supervisors Hilton Kobus and Joe Shapter for their supervision and guidance. In particular I would like to give a special thanks to my primary supervisor, Amanda Ellis for her encouragement, patience, and for believing in me over the last few years during this research. Your positive attitude and strong work ethic towards research in science has moulded me into the confident researcher I am today. I am certain that your wealth of knowledge, constructive criticism, and constant strive for excellence has made the last few years possible, it has been a great pleasure to be your student.

I must thank members of the ever changing Ellis research group, staff and academia at Flinders University, and members of the Flinders Centre for NanoScale Science and Technology, for their help, support, and amity over the past years.

Thanks to Kez, as a colleague, travel buddy and good friend. Jade, my bestie thanks for your mental-moral support and advice. Additional shout outs to Christine (my lunch buddy), Praveen, Luke, Bloky, Ra, Jess, Claire, Tony, Marky, Taryn, and Lee-Ann.

Finally I would like to thank my family in Adelaide and Darwin for their love, support (financially and mentally) and patience, which has always helped me towards achieving my goals. Love you all xo.

## Abstract

Over the last decade interest in fluorescent nanoparticles for forensic applications has greatly increased. This thesis describes the synthesis of fluorescent nanoparticles with polymer grafted from their surface for latent fingerprint detection. This allows for essential colour contrast for fingerprint visualisation and subsequent person identification.

In the first part of the thesis cadmium sulfide (CdS) quantum dots (QDs) were synthesised. These QDs have size tuneable fluorescence, which was investigated using theoretical calculations of band gap energies measured by UV-visible spectrophotometry. Once synthesised a chain transfer agent (CTA) was immobilised onto the QD surface using a Steglich esterification method. Subsequently reversible addition fragmentation chain transfer (RAFT) polymerisation (a controlled polymerisation technique), was used to graft dimethylacrylamide (DMA) from the surface of the QDs *via* the CTA on its surface. This gave a CdS/p(DMA) nanocomposite, which was water soluble. Aqueous solutions of CdS/p(DMA) were then applied as a solution reagent to successfully detect latent fingerprints deposited on non-porous substrates. The fluorescently developed fingerprints were visualised and photographed using a Polilight® (UV = 350 nm).

The RAFT process was versatile in that different monomers could be used, and hence different polymers with suitable physical attributes were synthesised. Random copolymers of DMA with methyl methacrylate (MMA) and styrene (Sty) were then grafted from the CdS QDs to give CdS/p(DMA-*co*-MMA) and CdS/p(DMA-*co*-Sty). This ultimately led to the synthesis of fluorescent powders that could be dusted onto the latent fingerprints for detection. The powders were found to give better ridge definition than the solution form.

Despite protection of the CdS QDs in the core of the polymers synthesised, there was always a residual concern for the use of the heavy metal, Cd, in the synthesis of these and other conventional QDs. Over the past decade years, research into nanocarbons has grown

exponentially, with our interest particularly focused on using fluorescent carbon nanoparticles (C-dots) for this thesis. C-dots, in literature, have been reported as non-toxic, biocompatible, alternatives to conventional QDs. C-dots were synthesised *via* thermal oxidation of activated charcoal (AC) in nitric acid. They were inexpensive to synthesise. Their optical properties were visually comparable to the CdS QDs, and emission intensities were found to be defined by working pH (acidity/basicity). We applied the same polymerisation techniques (RAFT) to synthesise C-dot/polymer nanocomposites to successfully detect latent fingerprints that were deposited on non-porous materials. Visually, these were comparable to the QD/polymer nanocomposites previously synthesised and applied successfully to the detection latent fingerprint on non-porous surfaces.

Lastly, the RAFT process was further exploited - by which the active end group (given by the RAFT agent) of the polymer was modified in a straightforward manner. Divinyl sulfone (DVS) modified magnetic beads were attached to CdS and C-dot polymer nanocomposites *via* a one-pot aminolysis/thiol-ene click reaction. This resulted in a magnetic fluorescent CdS QD or C-dot polymer powder that could potentially be used as a type of "Magna Powder" in latent fingerprint detection.

# Publications

## Journal articles

Dilag, J., Kobus, H., Ellis, A.V., CdS/polymer nanocomposites synthesised *via* surface initiated RAFT polymerization for the fluorescent detection of latent fingerprints. *Forensic Science International*, **228**, 105 (2013).

Dilag, J., Kobus, H., Ellis, A.V., Nanotechnology as a new tool for fingerprint detection: A review. *Current Nanoscience*, **7**, 153 (2011).

## Conference/Symposia proceedings

Dilag, J., Kobus, H., Yu, Y., Gibson, C., Shapter, J.G., Ellis, A.V., Quantum dot and carbon dot polymer nanocomposites for latent fingerprint detection, *RACI SA Student Polymer & Bionanotechnology Symposium*, Adelaide, SA, Australia, October 2013.

Dilag, J., Kobus, H., Yu, Y., Gibson, C., Ellis, A.V., Fluorescent carbon dots for latent fingerprint detection, *Centre for Nanoscale Science and Technology, 3<sup>rd</sup> Annual Symposium*, Adelaide, SA, Australia, July 2013.

Dilag, J., Kobus, H., Ellis, A.V., Forensic Nanotechnology, Forensic Nanotechnology: Synthesis and Application of Innovative Materials for Fingerprint Detection, *The 21<sup>st</sup> International Symposium on the Forensic Sciences*, Hobart, TAS, Australia, September 2012.

Dilag, J., Kobus, H., Ellis, A.V., New fluorescent nanocomposites for fingerprint detection, *33<sup>rd</sup> Australasian Polymer Symposium*, Hobart, TAS, Australia, February 2012.

Dilag, J., Kobus, H., Ellis, A.V., Quantum dots as a new tool for latent fingerprint detection, *APMC10/ICONN2012/ACMM22*, Perth, WA, Australia, February 2012.

Dilag, J., Kobus, H., Allan, K.E., D.A., Khodakov, Ellis, A.V., Nanotechnology: New materials for fingerprint detection & current advances in DNA analysis *Invited Speaker at Ecole de Sciences Criminelles, Institut de Police Scientifique*, University of Lausanne, Lausanne, Switzerland, July 2011.

Dilag, J., Kobus. H., Ellis, A.V., Quantum Dots Functionalised with Polymers *via* RAFT Polymerisation for the Fluorescent Detection of Latent Fingerprints, *European Polymer Congress*, Granada, Spain. June 2011.

Dilag, J., Kobus. H, Ellis, A.V., Synthesis of CdS/PDMA nanocomposites *via* surface initiated RAFT polymerisation for fingermark detection, *The 32<sup>nd</sup> Australasian Polymer Symposium*, Coffs Harbour, NSW, Australia, February 2011.

Dilag, J. Kobus, H., Ellis, A.V., Nanotechnology as a new tool for fingerprint detection, *The 20<sup>th</sup> International Symposium on the Forensic Sciences*, Sydney, NSW, Australia, September 2010.

Dilag, J., Kobus, H., Ellis, A.V., Nanotechnology as a new tool for fingerprint detection, *Australian Research Network for Advanced Materials and the Australian Research Council Network for Nanotechnology (ARNAM/ARCNN) Joint Workshop*, Adelaide, SA, Australia, June 2010.

## List of Figures

Figure 1.1. Energy level diagram of (a) a bulk semi-conductor with continuous energy bands and (b) a QD with discrete energy levels and larger band gap energy. ....	36
Figure 1.2. Energy level diagram showing a broad absorption and the narrow fluorescence emission characteristic of $E_{g(QD)}$ . Image adapted from [74]. ....	37
Figure 1.3. UV-vis absorption spectrum of aqueous CdS QDs with an absorption onset of 439 nm [77]. ....	39
Figure 1.4. Electronic structure of a QD with electron and electron hole traps [74]. ...	41
Figure 1.5. Absorption (solid line) and fluorescence (dashed line) spectra of colloidal CdS (20 mM), with the long-wavelength fluorescence magnified 40 times [74]. ....	41
Figure 1.6. Cyanoacrylate ester-fumed fingermark on aluminium foil, (a) without CdS/PAMAM and (b) developed with CdS/G4.0 PAMAM nanocomposite (using a yellow filter)[89].	46
Figure 1.7. Optical micrograph of fingermarks under UV illumination on a silicon wafer developed using the CdSe/ZnS QDs stabilised with octadecaneamine (magnification not specified in literature) [91]. ....	48
Figure 1.8. Photograph of CdS-chitosan-Tergitol powder developed latent fingermarks with 450 nm and (a) 550 nm band pass barrier filter (b) 565 nm long pass barrier filter [92]. ...	49
Figure 1.9. Raman spectra of C-dots, MWCNTs, highly ordered pyrolytic graphite (HOPG), and microdiamond powder [101]. ....	51
Figure 1.10. A UV spectrum of hydrophilic C-dots made from thermal decomposition of 2-(2-aminoethoxy)ethanol citrate salt. Figure taken from [136]. ....	56
Figure 1.11. Overlaid fluorescence emission spectra of 1.9 nm C-dots at different excitation wavelengths of 290–380 nm. Figure from [116]. ....	57
Figure 1.12. Structure of thiocarbonylthio RAFT agent and intermediate form on radical addition (figure adapted from [150]). ....	62



Figure 2.1. Reaction scheme for the synthesis of CdS/2-mercaptoethanol QDs. ....	82
Figure 2.2. Reaction scheme for the immobilisation of C <sub>12</sub> CTA to CdS/2-mercaptoethanol QDs. .....	83
Figure 2.3. Reaction scheme for RAFT polymerisation of DMA, MMA and Sty monomers from CdS/C <sub>12</sub> CTA QDs.....	85
Figure 2.4. One pot aminolysis/thiol-ene click reaction of C-dot and CdS/p(DMA- <i>co</i> -MMA) to DVS-magnetic beads. ....	90
Figure 2.5. Calibration curve for the integrated fluorescence versus measured absorbance of the dye R6G ( $y = 1958 x$ , $R^2 = 0.97383$ ).....	95
Figure 2.6. GPC calibration curve of PS standards.....	102
Figure 3.1. Synthesis of CdS/2-mercaptoethanol.....	108
Figure 3.2. Absorbance spectra of (a) bulk CdS and (b) CdS/2-mercaptoethanol QDs.....	110
Figure 3.3. Absorbance spectra of (I) CdS/2-mercaptoethanol QDs synthesised using equal ratio of precursors CdCl <sub>2</sub> : Na <sub>2</sub> S and (II) first derivative of spectra (I).....	111
Figure 3.4. Overlaid UV-vis spectra of CdS/2-mercaptoethanol QDs with varied CdCl <sub>2</sub> :Na <sub>2</sub> S concentrations of (a) 1:2, (b) 1:1 and (c) 2:1. ....	112
Figure 3.5. TEM image of CdS/2-mercaptoethanol QDs at 200 000 x magnification.....	114
Figure 3.6. Histogram of CdS/2-mercaptoethanol QD diameter measured from TEM imaging (n = 30). ....	115
Figure 3.7. Fluorescence emission spectrum of CdS/2-mercaptoethanol QDs in DMF using an excitation wavelength of 350 nm (averaged 50 scans). ....	115
Figure 3.8. Reaction scheme for immobilisation of C <sub>12</sub> CTA to CdS/2-mercaptoethanol QDs to give CdS/C <sub>12</sub> CTA QDs. ....	117
Figure 3.9. Mechanism for the DCC coupling reaction between CdS/2-mercaptoethanol QDs and C <sub>12</sub> CTA (I) Initial activation of C <sub>12</sub> CTA with DCC and (II) esterification between the activated C <sub>12</sub> CTA and CdS/2-mercaptoethanol.....	119

Figure 3.10. Mechanism for the role of DMAP in accelerating the esterification from 120	
Figure 3.11. Stacked FTIR spectra of (a) CdS/2-mercaptoethanol QDs and (b) CdS/C <sub>12</sub> CTA QDs. .....	122
Figure 3.12. TGA thermograms for (a) CdS/2-mercaptoethanol QDs (solid line) and (b) CdS/C <sub>12</sub> CTA QDs.....	124
Figure 3.13. Overlaid fluorescence spectra of (a) CdS/2-mercaptoethanol QDs and (b) CdS/C <sub>12</sub> CTA QDs.....	125
Figure 3.14. Scheme for the synthesis of CdS/p(DMA) nanocomposite <i>via</i> surface initiated RAFT polymerisation of DMA from CdS/C <sub>12</sub> CTA QDs.....	128
Figure 3.15. Overlaid <sup>1</sup> H NMR spectra of CdS/p(DMA) at (a) t = 0 h, (b) t = 48 h and (c) isolated CdS/p(DMA) upon precipitation in excess diethyl ether. Solvent: CDCl <sub>3</sub> . ..	133
Figure 3.16. FTIR spectra of CdS/p(DMA) at (a) t = 0 h and(b) purified CdS/p(DMA).134	
Figure 3.17. Scheme for the synthesis of (a) CdS/p(DMA- <i>co</i> -MMA) and (b) CdS/p(DMA- <i>co</i> -Sty) <i>via</i> initiated RAFT polymerisation of DMA, MMA and Sty from CdS/C <sub>12</sub> CTA QDs.136	
Figure 3.18. Kinetic plots of Ln[M <sub>0</sub> ]/[M] <sub>t</sub> versus time, for (■) p(DMA), (□) p(DMA- <i>co</i> -MMA) and (○) p(DMA- <i>co</i> -Sty) grafted from CdS/C <sub>12</sub> CTA QDs. ....	142
Figure 3.19. TGA thermograms of (i): (a) CdS/p(DMA), (b) CdS/p(DMA- <i>co</i> -MMA) and (c) CdS/p(DMA- <i>co</i> -Sty); and (ii): (d) p(DMA), (e) p(DMA- <i>co</i> -MMA) and (f) p(DMA- <i>co</i> -Sty). 144	
Figure 3.20. UV-vis absorbance spectra of (a) CdS/C <sub>12</sub> CTA QDs, (b) CdS/p(DMA), (c) CdS/p(DMA- <i>co</i> -MMA) and (d) CdS/p(DMA- <i>co</i> -Sty) in DMF, at an excitation of 350 nm. 146	
Figure 3.21. Fluorescence emission spectra of (a) CdS/C <sub>12</sub> CTA QDs, (b) CdS/p(DMA), (c) CdS/p(DMA- <i>co</i> -MMA) and (d) CdS/p(DMA- <i>co</i> -Sty) in DMF, at an excitation of 350 nm. 147	
Figure 4.1. Synthesis of C-dots <i>via</i> thermal oxidation of AC.....	155
Figure 4.2. Stacked Raman spectra of (a) AC, (b) C-dots, (c) pure KNO <sub>3</sub> and (d) KNO <sub>3</sub> salt removed from C-dot product.....	156
Figure 4.3. <sup>13</sup> C NMR spectrum of C-dots in D <sub>2</sub> O.....	158

Figure 4.4. Stacked FTIR spectra of (a) AC and (b) purified C-dots. ....	159
Figure 4.5. Stacked XPS survey scans of (a) AC and (b) purified C-dots.....	160
Figure 4.6. Size distribution histogram of C-dots determined by DLS. ....	162
Figure 4.7. Proposed chemical structure of C-dots with an oxidised surface. ....	163
Figure 4.8. Stacked UV-vis absorbance spectra of (a) HNO <sub>3</sub> , (b) NaNO <sub>3</sub> salt extracted and (c) NaOH. All solutions were prepared in Milli-Q water, with Milli-Q water baselines. ....	164
Figure 4.9. Stacked UV-vis absorbance spectra of (a) unneutralised C-dots, (b) neutralised C-dots and (c) purified carbon dots. Solutions were prepared in Milli-Q water, with Milli-Q water baselines.....	165
Figure 4.10. Overlaid fluorescence emission spectra of (a) HNO <sub>3</sub> , (b) NaNO <sub>3</sub> , (c) NaOH, (d) unneutralised C-dots, (e) neutralised C-dots and (f) purified C-dots (dashed line). Solutions were prepared in Milli-Q water with an excitation of 350 nm. ....	166
Figure 4.11. Fluorescence spectra of C-dots (in Milli-Q water) excited at (a) 350 nm, (b) 375nm (c) 400 nm, (d) 425 nm, (e) 450 nm and (f) 475 nm.....	168
Figure 4.12. Relative fluorescence intensity of the purified C-dots over 3 cycles of consecutively increasing and decreasing pH. pH range of 1 to 14. Excited at 350 nm. ....	170
Figure 4.13. Reaction scheme C-dot surface modification and grafting of DMA from C-dot surface using SI RAFT polymerisation.....	172
Figure 4.14. FTIR spectra of (a) purified C-dots (dashed line), (b) C-dot/C <sub>12</sub> CTA and (c) C-dot/p(DMA) nanocomposite. ....	173
Figure 4.15. TGA thermograms for (a) AC, (b) purified C-dots, (c) NaNO <sub>3</sub> salt by-product, (d) C-dot/C <sub>12</sub> CTA and (e) C-dot/p(DMA) nanocomposite. Under N <sub>2</sub> at a 10 °C min <sup>-1</sup> ramp rate. ....	174
Figure 4.16. <sup>1</sup> H NMR spectra of C-dot/p(DMA) nanocomposite at reaction times (a) t = 0 h and (b) t = 48 h. Solvent used was DMSO-d <sub>6</sub> .....	176
Figure 4.17. <sup>1</sup> H NMR spectra of C-dot/p(DMA) nanocomposite at t = 48, between 4 ppm and 0 ppm. Solvent used was DMSO-d <sub>6</sub> .....	176

Figure 4.18. Kinetic plot for the polymerisation of DMA from C-dot/C <sub>12</sub> CTA via RAFT polymerisation.....	178
Figure 4.19. Overlaid UV-vis absorbance spectra of (a) C-dots, (b) C-dots/C <sub>12</sub> CTA and (c) C-dots/p(DMA).....	179
Figure 4.20. Overlaid fluorescence emission spectra of (a) C-dots, (b) C-dot/C <sub>12</sub> CTA and (c) C-dot/p(DMA) nanocomposite. ....	180
Figure 5.1. Synthesis of magnetic CdS/p(DMA-co-MMA)* and C-dot/p(DMA-co-MMA)* nanocomposites via a one-pot aminolysis/thiol-ene click reaction. The sphere in the scheme represents either CdS QDs or C-dots and the oval represents the iron microparticle (not to scale). .....	186
Figure 5.2. Chemical structure of CdS/p(DMA-co-MMA) or C-dot/p(DMA-co-MMA) with the RAFT end-group highlighted in the dotted box.....	188
Figure 5.3. Structures of possible side products of simultaneous aminolysis/thiol-ene click reaction and aminolysis only as a result of using trithiocarbonate C <sub>12</sub> CTA used in this research. .....	189
Figure 5.4. FTIR spectra of (a) DVS-magnetic beads, (b) magnetic p(DMA-co-MMA)* and (c) magnetic C-dot/p(DMA-co-MMA)* nanocomposites.....	191
Figure 5.5. Overlaid TGA thermograms of (a) DVS-magnetic beads, (b) CdS/p(DMA-co-MMA), (c) C-dot/p(DMA-co-MMA), (d) magnetic CdS/p(DMA-co-MMA)* and (e) magnetic C-dot/p(DMA-co-MMA)*.....	194
Figure 5.6. Overlaid UV-vis absorbance spectra of (a) DVS-magnetic beads, (b) CdS/p(DMA-co-MMA), (c) C-dot/p(DMA-co-MMA), (d) magnetic CdS/p(DMA-co-MMA)* and (e) magnetic C-dot/p(DMA-co-MMA)*.....	197
Figure 5.7. Overlaid fluorescence emission spectra of (a) DVS-magnetic beads, (b) CdS/p(DMA-co-MMA), (c) C-dot/p(DMA-co-MMA), (d) magnetic CdS/p(DMA-co-MMA)* and (e) magnetic C-dot/p(DMA-co-MMA)*, in DMF, excited at 350 nm.....	199

Figure 5.8. Stacked fluorescence emission spectra of (a) DVS-magnetic beads, (b) CdS/p(DMA- <i>co</i> -MMA)* and (c) C-dot/p(DMA- <i>co</i> -MMA)* using an excitation of 350 nm.....	201
Figure 5.9. Photographs of magnetic CdS/p(DMA- <i>co</i> -MMA)* on a magnetic rod under (a) white light and (b) UV illumination in a dark room (shutter speed = 30 s).....	202
Figure 6.1. The emission spectrum of a high pressure xenon arc lamp used in the Polilight®. Image scanned from Australian Federal Police workshop booklet [6]. .....	209
Figure 6.2. Main classification patterns (a) arch, (b) loop and (c) whorl (image was taken from the Australian police website <a href="http://www.australianpolice.com.au/dactyloscopy/fingerprint-pattern-classification/">http://www.australianpolice.com.au/dactyloscopy/fingerprint-pattern-classification/</a> . visited 2012). .....	212
Figure 6.3. Fingerprint annotated with the different types of minutiae that can be identified [4]. .....	212
Figure 6.4. Camera and Polilight® setup for latent fingerprint visualisation and photography.	216
Figure 6.5. Latent fingerprints on aluminium foil developed by row (a) CdS/p(DMA) solution reagent, (b) CdS/p(DMA- <i>co</i> -MMA) powder, (c) CdS/p(DMA- <i>co</i> -Sty) powder, (d) C-dot/p(DMA) solution reagent and (e) C-dot/p(DMA- <i>co</i> -MMA) powder. Photographs were taken under UV illumination (350 nm) using no filter, a green filter (555 ± 24 nm) and a red filter (640 ± 40 nm) as annotated. Left fingerprint: fresh latent fingerprints, right fingerprint: aged fingerprints.	218
Figure 6.6. Latent fingerprints on glass microscope slides developed by row (a) CdS/p(DMA- <i>co</i> -MMA), (b) CdS/p(DMA- <i>co</i> -Sty) and (c) C-dot/p(DMA- <i>co</i> -MMA). Photographs were taken under UV illumination (350 nm) using no filter, a green filter (555 ± 24 nm) and red filter (640 ± 40 nm). Left fingerprint: fresh latent fingerprints, right: aged fingerprints. ....	224
Figure 6.7. Photographs of latent fingerprints deposited on (a) aluminium foil and (b) glass microscope slide developed by the magnetic CdS/p(DMA- <i>co</i> -MMA)* powder. Photographs were taken under UV illumination (350 nm) with a blue filter (450 ± 80 nm). .....	227
Figure 8.1. <sup>1</sup> H NMR spectra of CdS/p(DMA- <i>co</i> -MMA) in CDCl <sub>3</sub> .....	242
Figure 8.2. <sup>1</sup> H NMR spectra of CdS/p(DMA- <i>co</i> -MMA) in CDCl <sub>3</sub> .....	242

Figure 8.3. Normalised fluorescence intensity, peak maxima position of CdS/p(DMA) in DMF aged over 0, 2, 6, 12, and 18 months. (Excitation of 350 nm). ..... 243

## List of Tables

Table 1.1. Location and components of sweat excreted from the eccrine apocrine and sebaceous glands [5, 7]. .....	30
Table 3.1. Values for absorption onset, $E_g$ (eV) and estimated diameter (nm) of CdS QDs synthesised calculated from Figure 3.4.....	113
Table 3.2. Calculated values of residue, $T_d$ as a range and weight loss after $T_d$ , from the TGA thermograms of CTA (a) CdS/p(DMA) and (b) CdS/p(DMA- <i>co</i> -MMA). .....	124
Table 3.3. $M_n$ , Conversion and PDI determined by GPC and $^1H$ NMR spectroscopy of synthesised by conventional polymerisation and RAFT polymerisation. ....	131
Table 3.4. Monomer ratio consumed in polymerisation monomer conversion, $M_n$ and PDI values calculated for polymers grafted from CdS QDs; p(DMA), p(DMA- <i>co</i> -MMA) and p(DMA- <i>co</i> -Sty), respectively.....	140
Table 3.5. Calculated values of residue, $T_d$ as a range and weight loss after $T_d$ , from the TGA thermograms of CTA (a) CdS/p(DMA), (b) CdS/p(DMA- <i>co</i> -MMA) and (c) CdS/p(DMA- <i>co</i> -Sty), and RAFT polymers without CdS QDs; (d) p(DMA), (e) p(DMA- <i>co</i> -MMA) and (f) p(DMA- <i>co</i> -Sty).....	144
Table 3.6. Maximum fluorescence, fluorescence intensity and FWHM recorded for (a) CdS/C <sub>12</sub> CTA QDs, (b) CdS/p(DMA), (c) CdS/p(DMA- <i>co</i> -MMA) and (d) CdS/p(DMA- <i>co</i> -Sty) in DMF, at an excitation of 350 nm. ....	147
Table 3.7. Calculated QY for CdS/polymer nanocomposites. ....	149
Table 4.1. Peak position, peak area (%), FWHM and At % values calculated from the XPS analysis of (a) AC and (b) C-dots (Figure 4.4 (a) and (b)). .....	161
Table 4.2. The maximum fluorescence emission intensity and FWHM determined from the fluorescence emission spectra (Figure 4.10) of (d) unneutralised C-dots (e) neutralised C-dots and (f) purified C-dots. ....	167

Table 4.3. Fluorescence peak maxima and intensity measured for purified C-dots excited at 350 nm, 400 nm, 425 nm, and 450 nm. ....	168
Table 4.4. Maximum fluorescence wavelength, fluorescence intensity and FWHM recorded from the fluorescence emission spectra of (a) C-dots, (b) C-dot/C <sub>12</sub> CTA and (c) C-dot/p(DMA) nanocomposite. Data normalised to the C-dot fluorescence spectrum (Figure 4.20 (a)).	180
Table 5.1. Values for wt/wt % residue after heating to 500 °C, T <sub>d</sub> as a range, T <sub>d</sub> and wt/wt % maximum weight loss after T <sub>d</sub> . ....	195
Table 5.2. Measured absorbance wavelength at absorbance = 0.5 a.u for samples (a) DVS-magnetic beads, (b) CdS/p(DMA-co-MMA), (c) C-dot/p(DMA-co-MMA), (d) magnetic CdS/p(DMA-co-MMA)* and (e) magnetic C-dot/p(DMA-co-MMA)*. ....	198
Table 5.3. Fluorescence maxima, intensity, FWHM and QY % of (a) DVS-magnetic beads, (b) CdS/p(DMA-co-MMA), (c) C-dot/p(DMA-co-MMA), (d) magnetic CdS/p(DMA-co-MMA)* and (e) magnetic C-dot/p(DMA-co-MMA)*. ....	199
Table 6.1. Band characteristics of a typical Polilight <sup>®</sup> (model PL10 used in this thesis, table adapted from [6]). ....	210
Table 6.2. Preparation and application of the CdS QD and C-dot polymer nanocomposite fingerprint reagents. ....	215
Table 6.3. Summary of the performance of CdS QD and C-dot polymer nanocomposites fingerprint reagents. ....	229



## Lists of abbreviations, symbols and units

Symbol/acronym/unit	Translation/explanation
$\Omega$	Ohms
$\hbar$	The Dirac constant
$\delta$	Chemical shift
%	Per cent
$^{13}\text{C}$ NMR	Carbon 13 nuclear magnetic resonance spectroscopy
$^1\text{H}$ NMR	Proton nuclear magnetic resonance spectroscopy
a.u	Arbitrary units
AC	Activated charcoal/carbon
AF	Autofocus
AIBN	Azobisisobutyronitrile
Al	Aluminium
Ar	Aromatic ring
C	Carbon
C=O	Carbonyl
C <sub>12</sub> CTA	C <sub>12</sub> chain transfer agent
Ca	Calcium
CDCl <sub>3</sub>	Deuterated chloroform (chloroform-d)
CdCl <sub>2</sub>	Cadmium chloride
C-dot	Carbon dot
CdS	Cadmium sulfide
CdSe	Cadmium selenium
cm <sup>-1</sup>	Wavenumber
COOH	Carboxylic acid
co	Co-polymer
cps	Counts per second
CTA	Chain transfer agent
Cu	Copper
D <sub>2</sub> O	Deuterated water
D-band	Disorder band
DCC	Dicyclocarbodiimide
°C	Degrees Celsius
DHU	Dicyclohexylurea
DMA	<i>N</i> - <i>n</i> -dimethylacrylamide
DMAP	4-dimethylaminopyridine
DMF	<i>N,N</i> -Dimethylformamide
DMSO-d <sub>6</sub>	Deuterated dimethylsulfoxide
DTP	2,2'- dithiodipyridine
DVS	Divinyl sulfone
Eg	Band gap energy
eV	Electron volts
FTIR	Fourier transform infra-red

<b>G</b>	Generation
<b>g mol<sup>-1</sup></b>	Grams per mole
<b>G-band</b>	Graphite band
<b>h</b>	Hour
<b>H<sub>2</sub>SO<sub>4</sub></b>	Sulfuric acid
<b>HNO<sub>3</sub></b>	Nitric acid
<b>HPLC</b>	High performance/pressure liquid chromatography
<b>I</b>	Intensity
<b>Ind-Zn</b>	1-2-indandione/zinc
<b>J</b>	Joule
<b>K</b>	Potassium
<b>Kg</b>	Kilogram
<b>L</b>	Litre
<b>λ</b>	Lambda (wavelength)
<b>M , mol L<sup>-1</sup></b>	Moles per litre
<b>MHz</b>	Mega Hertz
<b>min</b>	Minute
<b>mL</b>	Millilitre
<b>MMA</b>	Methyl methacrylate
<b>M<sub>N</sub></b>	Molecular weight number average
<b>M<sub>w</sub></b>	Molecular weight
<b>mW</b>	Mega Watts
<b>MWCNT</b>	Multiwalled carbon nanotubes
<b>N or N<sub>2</sub></b>	Nitrogen
<b>Na</b>	Sodium
<b>Na<sub>2</sub>S</b>	Sodium sulfide
<b>NaBH<sub>4</sub></b>	Sodium borohydride
<b>NaCl</b>	Sodium chloride
<b>nano</b>	Nanometer
<b>NaNO<sub>3</sub></b>	Sodium nitrate
<b>NaOH</b>	Sodium hydroxide
<b>Nd</b>	neodymium
<b>nm</b>	Nanometer
<b>O</b>	Oxygen
<b>OH</b>	Hydroxyl
<b>p</b>	Poly- (e.g., p(DMA) = poly(dimethylacrylamide))
<b>PAGE</b>	Polyacrylamide gel electrophoresis
<b>PAMAM</b>	Polyamidoamine
<b>PDI</b>	Polydispersity index
<b>PEG</b>	Polyethylene glycol
<b>Ph</b>	Phenyl
<b>pH</b>	Power of Hydrogen (per Hydrogen)
<b>π</b>	Pi
<b>PPE</b>	Personal protective equipment
<b>ppm</b>	Parts per million
<b>QD</b>	Quantum dot

<b>QY</b>	Quantum yield
<b>r</b>	Radius
<b>R6G</b>	Rhodamine 6G
<b>RAFT</b>	Reversible addition fragmentation chain transfer
<b>RT</b>	Room temperature
<b>S</b>	Sulfur
<b>s</b>	Second
<b>Si</b>	Silicon
<b>σ</b>	Sigma
<b>SIP</b>	Surface initiated polymerisation
<b>sp</b>	Sharp principle orbital
<b>Sty</b>	Styrene
<b>T<sub>d</sub></b>	Degradation temperature
<b>TEM</b>	Transmission electron microscopy
<b>TGA</b>	Thermal gravimetric analysis
<b>UV</b>	Ultra violet
<b>UV-vis</b>	Ultra violet-visible
<b>V</b>	Volts
<b>wt/wt %</b>	Weight per weight per cent
<b>Xe</b>	Xenon
<b>YAG</b>	yttrium aluminium garnet
<b>ZnS</b>	Zinc sulfide

# Thesis Guide

Chapter #	Short description
1	Introduction: Background information about the significance of latent fingerprint detection, and conventional methods of detection, quantum dots (QDs) including a literature review of QDs in latent fingerprint detection, carbon dots, reversible addition fragmentation chain transfer (RAFT) polymerisation and RAFT end-group removal/modification.
2	Experimental methods: Details pertaining to the synthesis and characterisation of Cd QD and C-dot polymer nanocomposites and magnetic CdS and C-dot polymer nanocomposites.
3	CdS/polymer nanocomposites: Describes the synthesis and characterisation of the CdS QDs used for the synthesis of CdS/polymers: CdS/p(DMA), CdS/p(DMA- <i>co</i> -MMA) and CdS/p(DMA- <i>co</i> -Sty) <i>via</i> surface initiated RAFT polymerisation.
4	C-dot/polymer nanocomposites: Describes the synthesis and characterisation of the C-dots used for the synthesis of C-dot/polymer: C-dot/p(DMA) <i>via</i> surface initiated RAFT polymerisation.
5	RAFT end group modification: The synthesis of magnetic CdS/p(DMA- <i>co</i> -MMA) and C-dot/p(DMA- <i>co</i> -MMA) – describes the synthesis of these magnetic nanocomposites <i>via</i> a one-pot aminolysis/thio-lene click chemistry reaction.
6	Application of CdS QD and C-dot polymer nanocomposites to latent fingerprint detection: Describes the preparation and application of the synthesised nanocomposites from Chapters 3, 4, and 5 to latent fingerprint detection. This chapter will contain its own introduction and experimental sections describing the preparation of latent fingerprints, the CdS and C-dot polymer nanocomposites as reagents for fingerprint detection.
7	Conclusions and future directions: Concluding remarks on the research presented in the thesis, and potential research projects related to the research presented.